

RECENT STUDIES OF PHASE EQUILIBRIA AT HIGH PRESSURES

G.M. SCHNEIDER

Physical Chemistry Laboratory, Department of Chemistry, University  
of Bochum, D - 4630 Bochum 1, Federal Republic of Germany

ABSTRACT

In its first part the present review considers the dependence of phase transition temperatures of some selected liquid crystals on pressure up to 300 MPa with differential thermal analysis (DTA) and diamond anvil techniques; here also pressure-induced phases as well as tricritical and reentrant phenomena will be discussed. In the second part the most important types of high-pressure phase diagrams of fluid mixtures are shortly reviewed. Here recent results on binary systems (containing trifluoromethane, tetrafluoromethane, nitrogen etc) will be presented and compared with data that are calculated from an equation of state. The results will be discussed in relation to some applications e.g. in fluid extraction and supercritical fluid chromatography (SFC).

INTRODUCTION

The present review considers the approach to the isotropic liquid state on two different ways both involving high pressures: the first (for a pure component) starting at (relatively) low temperatures from a solid phase going via liquid crystalline states and the second (for binary mixtures) starting at (relatively) high temperatures in the supercritical one-phase region going via fluid-fluid phase equilibria and their related critical phenomena.

Fig.1 shows where these states are found in the pressure(p) - temperature(T) diagram of a pure substance. Here the solid phase  $s_1$ , the isotropic liquid phase l and the gaseous phase g as well as in addition a second solid phase  $s_2$  or a liquid crystalline phase (here nematic n) between  $s_1$  and l are considered.

The melting transition from a positionally and orientationally ordered solid  $s_1$  to the positionally and orientationally disordered isotropic liquid l is a direct one in most cases. But for many substances it is made via an additional high temperature solid phase (here  $s_2$ ) where the positional order of solid  $s_1$  is widely maintained whereas a considerable amount of orientational disorder exists (so-called plastic crystals). Investigations in this field

using microcalorimetric high-pressure techniques (e.g. DSC) will be treated in another contribution to these Proceedings (ref.1).

For a large and very important class of substances the melting transition is effectuated via anisotropic liquid crystalline states exhibiting different degrees of positional disorder where, however, a considerable amount of orientational order is remaining. Some results that have been recently obtained in the author's laboratory on some selected liquid crystals exhibiting nematic and smectic phases will be presented in the first part of this review. Here pressure-induced phases as well as tricritical and reentrant phenomena will also be considered. Liquid crystals are also treated in some other contributions to these Proceedings (see refs.2 and 3).

To higher temperatures the stability range of the isotropic liquid phase  $l$  is limited by the critical region; e.g. for a pure substance the vapour pressure curve ends at the critical point CP where the coexisting liquid and the gaseous phases become identical. In the second part of this review it will be pointed out how the critical parameters will be influenced by the addition of a second component. The most important types of phase diagrams of fluid binary mixtures at high pressures and the related critical phenomena will be shortly reviewed and some characteristic data will be presented that have been recently obtained in the author's laboratory. Here the accent will be on binary mixtures of a supercritical gas I with a low-volatile organic compound II. Such mixtures are of fundamental interest for some new separation methods (e.g. (supercritical) fluid extraction or extraction with dense gases, supercritical fluid chromatography (SFC)).

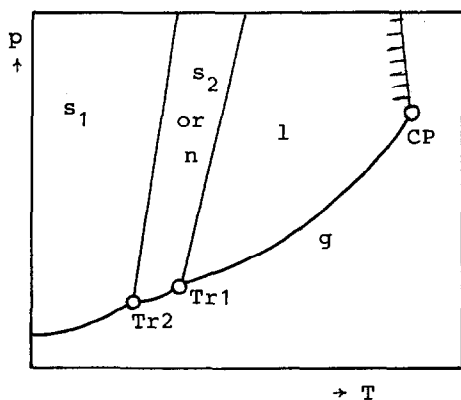


Fig. 1.  $p(T)$  phase diagram of a one-component system (schematic; see text;  $\text{||||}$  = critical  $p(T)$  curve of binary system)

## PHASE EQUILIBRIA OF LIQUID CRYSTALS AT HIGH PRESSURES

As temperature and additives, pressure is an important parameter to influence order and polymorphism of a liquid crystal. Therefore high pressure studies on the phase behaviour of liquid crystals have become of growing interest during the last years. A review of the activities and the progress in this field of experimental and scientific research has been given by Chandrasekhar and Shashidhar (ref. 4) some years ago.

In the following some results will be presented that are typical for the high-pressure phase behaviour of nematic and smectic liquid crystalline phases; they have been obtained recently in our laboratory with differential thermal analysis (DTA) and diamond anvil techniques (DAC). The older work performed in our laboratory has been reviewed elsewhere (ref. 11).

### Experimental Techniques

For the measurements differential thermal analysis (DTA) and diamond anvil cell techniques (DAC) were used both methods being complementary: With DAC phase transitions of higher order can also be observed that are not detectable by DTA whereas first order transition temperatures determined as a function of pressure by DTA can be used for the pressure calibration of the DAC equipment. For details see refs. 5 - 13.

Differential Thermal Analysis (DTA). The high-pressure autoclave used in the DTA experiments is shown in Fig. 2a. The pressure vessel is made from Nimonic 90 and is closed by a Bridgman piston. The steel-sheathed thermocouples are soldered into two blind plugs, which are screwed into the autoclave from below. The samples are encapsulated in lead, indium or nickel cells (Fig. 2b) to prevent the pressure transmitting argon gas from being dissolved in the sample.

Fig. 3 shows a schematic representation of the whole set-up. The autoclave is heated at a constant rate with an electrical regulator and pressurized with argon gas using a high-pressure pump. In the analog mode of operation (left hand side of Fig. 3) the (amplified) temperature difference  $\Delta T$  between reference and sample cell, the differentiated signal  $d\Delta T/dt$  as well as the temperature  $T$  of the reference cell are plotted against time  $t$  with a recorder. In the digital mode of operation (right hand side of Fig. 3) the data are recorded at equidistant time steps of about 750 ms with a microcomputer (hp 85) after analog/digital conversion. All computations (such as integration, differentiation, temperature measurement etc)

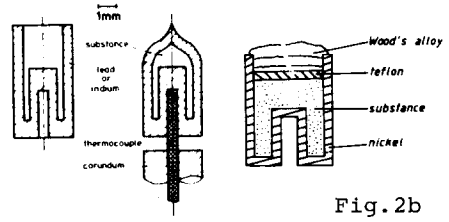
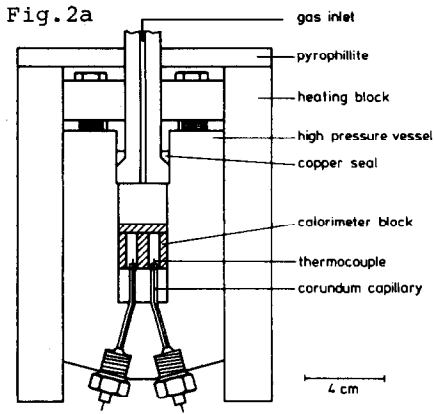


Fig. 2. High-pressure DTA (refs. 6,11)

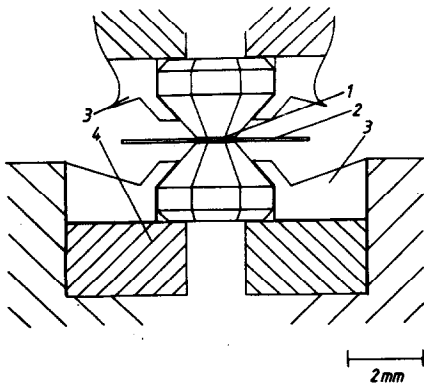
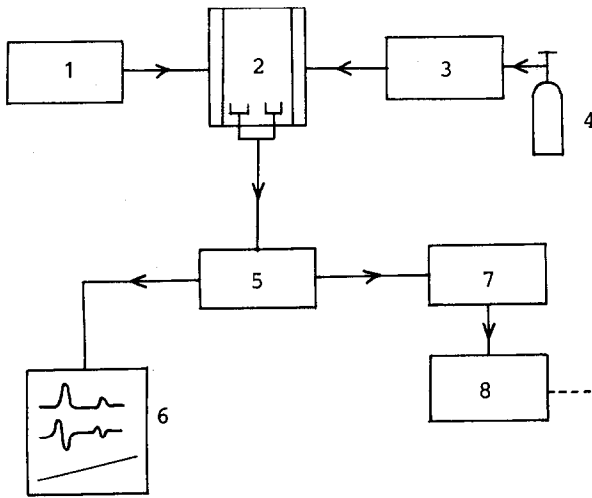


Fig. 4. Diamond anvil cell (principle; 1 sample, 2 gas-gasket, 3 brass ring, 4 steel support (refs. 5,11))

can be done offline with a desk-top computer (hp 9845). For details see refs. 6,8-11.

Diamond Anvil Cell (DAC). In the diamond anvil cell technique the sample is inserted between two diamonds, which are compressed mechanically by lever arms (Fig. 4). Hydrostatic pressure is obtained by using a gasket made from a foil of 0.1 mm thick hardened steel. The diamond anvil cell is adapted to a polarizing microscope making possible a detection of phases and phase transitions by direct optical observation; thus it was also possible to observe textures of liquid crystals under pressure in a diamond anvil cell for the first time. Additionally phase transitions are simultaneously monitored by recording the change of light intensity transmitted through the sample as a function of temperature and/or pressure. For details see refs. 5,7,11.

#### Results on Some Selected Liquid Crystals

In Figs. 5, 6 and 7 the  $p(T)$  phase diagrams are shown of the butyl (TBBA), the octyl (TBAA(8)) and the dodecyl (TBAA(12)) homologues of the terephthal-bis(4-n-alkylanilines) obtained from high-pressure DTA and DAC experiments up to about 3 kbar (refs. 7,8,12, 13). The substances exhibit a complex phase behaviour. For TBAA(8) the nematic phase (Fig. 6) and for TBAA(12) the smectic A phase (Fig. 7) are pressure-induced. The pressure-induced appearance of the nematic phase in TBAA(8) (Fig. 6) can easily be deduced from the splitting of the high-temperature peak in the original DTA traces for this substance with increasing pressures (see Fig. 8). For the  $smA/smC$  transition in TBAA(8) no normal DTA signals are found any longer for pressures exceeding about 1 kbar whereas it can be observed to even higher pressures by DAC; this behaviour indicates the existence of a so-called tricritical point where first order contributions in the phase transition vanish or are not longer detectable (Fig. 6). Thus Figs. 5-7 demonstrate the advantage in combining high-pressure DTA and DAC experiments in the investigation of liquid crystals. Besides the determination of the  $smA/n$  and  $n/l$  phase transition lines at pressures and temperatures beyond the experimental range of the DTA apparatus is also possible (e.g. Fig. 6). For a detailed discussion especially of the low-temperature transitions and the annealing behaviour see refs. 7,8,12,13.

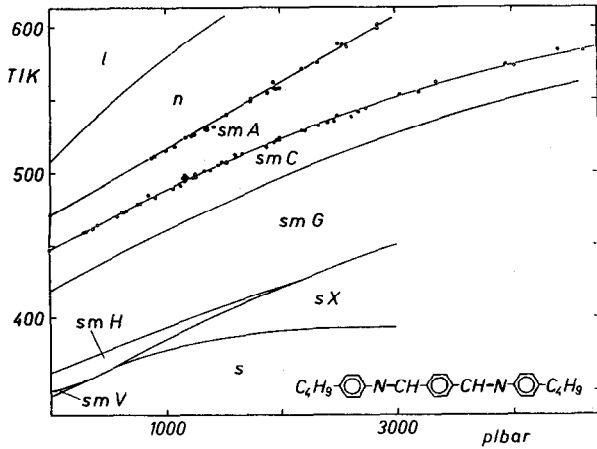


Fig. 5. T(p) phase diagram of TBBA (refs. 7,12)

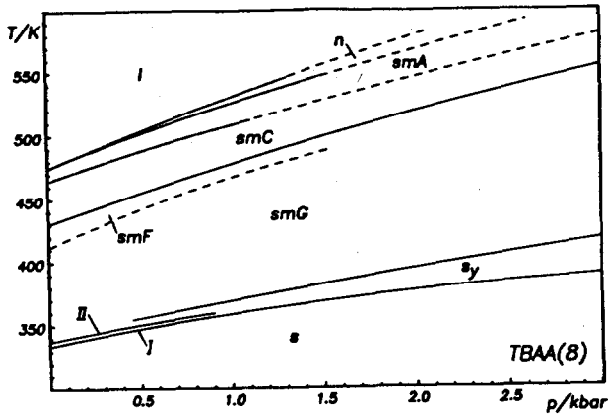


Fig. 6. T(p) phase diagram of TBAA(8) (refs. 7,8,13) (— DTA results; --- DAC results)

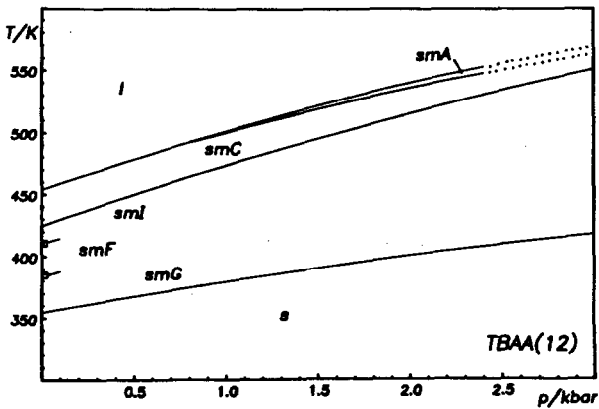


Fig. 7. T(p) phase diagram of TBAA(12) (refs. 8,13) (— DTA results; ... extrapolated data)

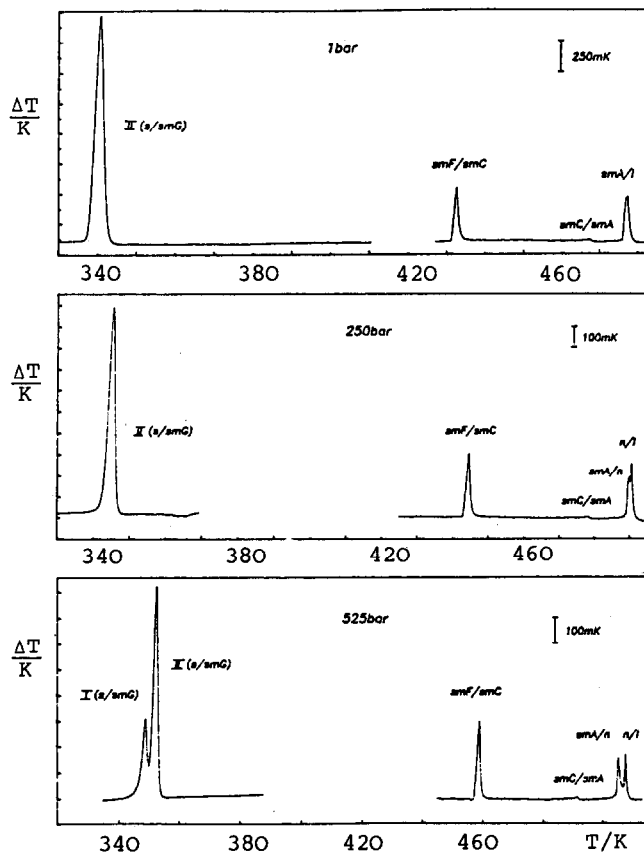


Fig. 8. DTA traces for TBAA(8) (ref. 8)

In Fig. 9 the improved resolution of DTA by using differentiated signals is demonstrated for 4-cyano-4'-nonyloxybiphenyl (9OCB): Whereas the normal signal is clearly visible at 1 bar (Fig. 9a), it is disappearing below the noise at 625 bar (Fig. 9b); the differentiated signals, however, remain detectable up to 1740 bar (Fig. 9c-f). The corresponding p(T) phase diagram of 9OCB is given in Fig. 10.

For a study of reentrant phenomena in 4-cyano-4'-octyloxybiphenyl (8OCB) and its binary mixtures with 4-cyanobenzyliden-4'-octyloxyaniline(CBOOA) by computerized high-pressure DTA see refs. 5,6,11.

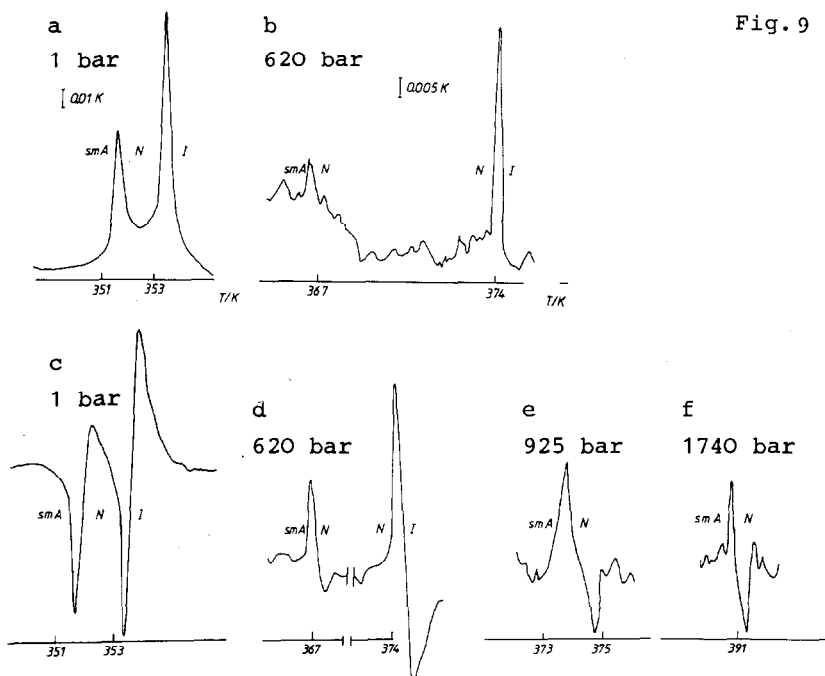


Fig. 9

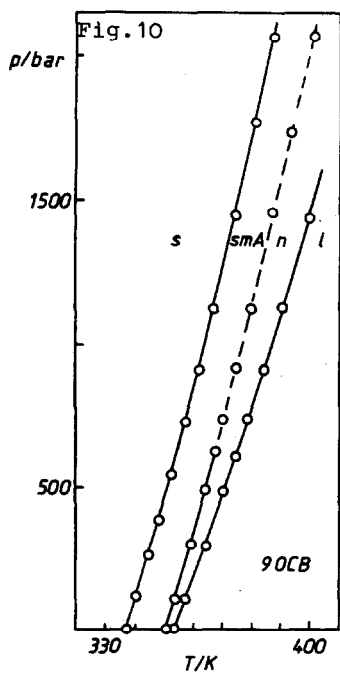


Fig. 9. DTA traces for the liquid crystal 90CB

a + b: normal signals

c - f: differentiated signals

Fig. 10:  $p(T)$  phase diagram of the liquid crystal 90CB

(— = detected from normal and differentiated signals

--- = detected from differentiated signals only)



## PHASE EQUILIBRIA AND CRITICAL PHENOMENA IN FLUID MIXTURES

### Phase-theoretical Aspects

Fluid mixtures, especially in the critical and supercritical regions, are becoming increasingly important in many fields. The physico-chemical aspects of these applications have been discussed in two books (refs.14 and 15), in the proceedings of several meetings or special issues of some journals (refs.16-20) and several review articles some of them written by the author (refs.21-26) where earlier reviews are also cited. It is the aim of this paper to give a short introduction to the phase-theoretical aspects of fluid mixtures on the basis of the earlier reviews.

In fluid mixtures three different types of two-phase equilibrium exist, namely liquid-liquid (ll), liquid-gas (lg) and gas-gas (gg) equilibria. In Fig.11 schematic pTx diagrams (upper row) and p(T) projections (lower row) are given for binary systems. Fig.11a characterizes a system with a critical curve lg being not interrupted and liquid-liquid phase separation (ll) at much lower temperatures, the upper critical solution temperature (UCST) decreasing (type 1) or increasing (type 2) slightly with pressure. In Fig.11b the critical curve ll is displaced to temperatures high enough that it may pass continuously into the critical curve lg. In Fig.11c no pressure minimum and maximum are found any longer on the critical curve. Systems showing a temperature minimum on the critical curve (e.g. type 3 in Fig.11b, type 2 in Fig.11c) or starting at CPII with a positive slope have to be attributed to gas-gas equilibria of the 2nd or 1st kind, respectively. For details and examples see refs. 21 - 26.

Thus Fig.11 shows that there are continuous transitions between ll, lg and gg equilibria. These transitions can be demonstrated by investigating so-called "families" of systems where one component is maintained constant whereas the other is systematically altered in size, shape, structure and/or polarity.

### Results on the System $\text{CHF}_3$ + Octane and the $\text{CHF}_3$ -Family

In Fig.12 some results for the fluid phase behaviour in the system  $\text{CHF}_3$  + octane are given; this system corresponds to type 3 in Fig.11b. The data have been obtained by Wirths (refs.27,28,31) according to the so-called synthetic method. In Fig.12a some p(T) curves for x = const (so-called isopleths) are given whereas in Fig.12b and 12c T(x) isobars and p(x) isotherms are shown, respectively; they have been obtained by interpolation from the p(T) iso-

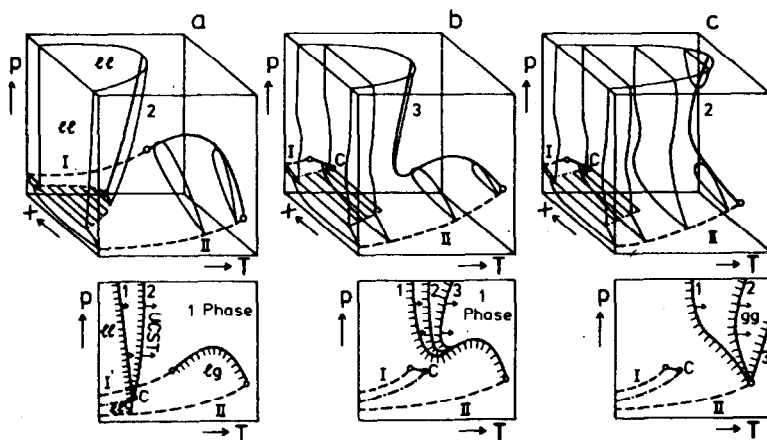


Fig. 11.  $pTx$  phase diagrams (upper row) and  $p(T)$  projections (lower row) of fluid binary mixtures (schematically; see text)  
 — =  $p(x)$  isotherm; — = critical curve of binary mixtures;  
 --- = vapour pressure curve of pure component; -.-.- = three-phase line  $llg$ ;  $o$  = critical point of pure component (CP);  $C$  = critical endpoint; UCST = upper critical solution temperature;  $lg$  = liquid-gas;  $ll$  = liquid-liquid;  $gg$  = gas-gas; for details see refs. 21-26

pleths in Fig. 12a.

The  $p(T)$  projection of the critical curve (being the envelope of the  $p(T)$  isopleths in Fig. 12a) is shown in Fig. 13 and compared with those of other  $CHF_3$  binaries. Whereas the branches of the critical curves shown for  $CHF_3 + CH_4$ ,  $CHF_3 + C_2H_6$  and  $CHF_3 + n-C_6H_{14}$  correspond to  $ll$  equilibria and resemble type 2 in Fig. 11a, all other systems have to be attributed to  $gg$  equilibria of the 2nd kind corresponding to type 3 in Fig. 11b or type 2 in Fig. 11c.

### Results on Other Families

A very similar continuity was demonstrated in other series of binary systems where a constant component I such as carbon dioxide, methane, ethane, ethylene, and water and more recently nitrogen (refs. 29-31), tetrafluoromethane (refs. 27,28,31) and sulphurhexafluoride (refs. 32-34) was combined with a component II that was systematically altered (e.g. within the series of the  $n$ -alkanes). In Figs. 14-16 some results on the tetrafluoromethane (refs. 27,28,31), sulphurhexafluoride (refs. 32-34) and nitrogen (refs. 29-31) families that have been recently obtained in the author's laboratory according to the synthetic (refs. 27-34) as well as

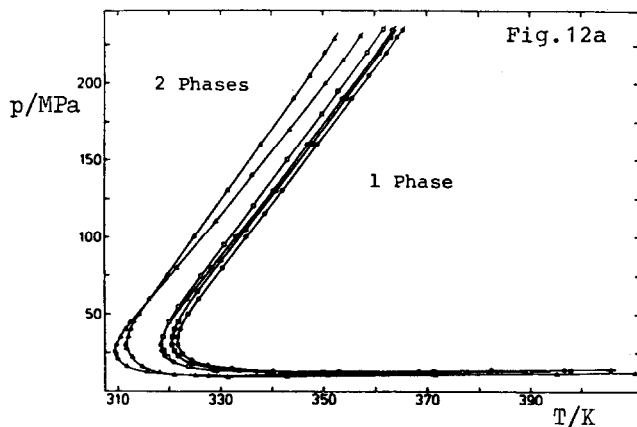
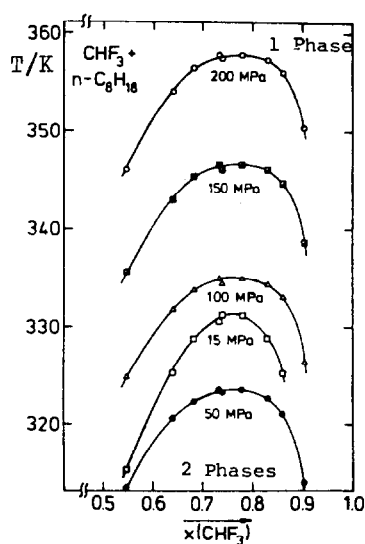


Fig. 12. Fluid phase equilibria in the system  $\text{CHF}_3 + \text{octane}$  (Wirths; refs.27,28)

Fig.12a.  $p(T)$  isopleths

Fig.12b.  $T(x)$  isobars

Fig.12c.  $p(x)$  isotherms



+ Fig.12b

Fig.12c +

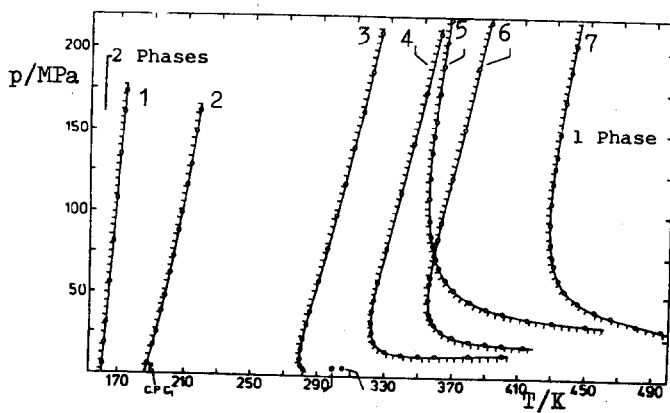
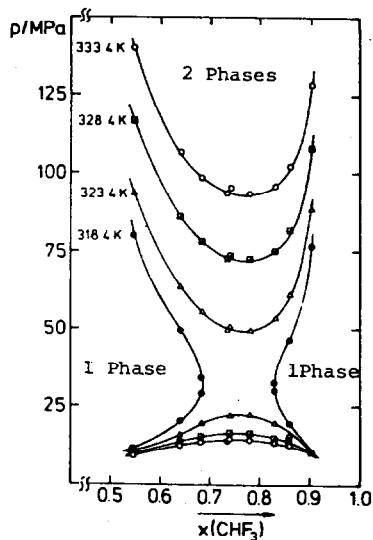


Fig. 13. Critical  $p(T)$  curves of binary  $\text{CHF}_3 + \text{hydrocarbon}$  systems (1= $\text{CHF}_3 + \text{CH}_4$ , 2= $\text{CHF}_3 + \text{C}_2\text{H}_6$ , 3= $\text{CHF}_3 + \text{n-C}_6\text{H}_{14}$ , 4= $\text{CHF}_3 + \text{n-C}_8\text{H}_{18}$ , 5= $\text{CHF}_3 + \text{C}_{10}\text{H}_{12}$  (tetralin), 6= $\text{CHF}_3 + \text{n-C}_{10}\text{H}_{22}$ , 7= $\text{CHF}_3 + \text{C}_{10}\text{H}_{18}$  (decalin, cis); Wirths; refs.27,28)

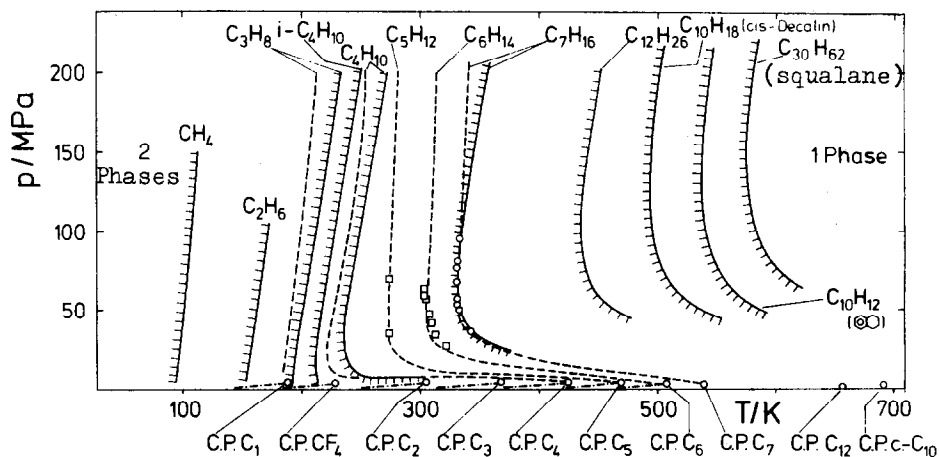


Fig. 14. Critical  $p(T)$  curves of some binary ( $\text{CF}_4$  + hydrocarbon) systems ( $\text{C}_n\text{H}_{2n+2}$  =  $n$ -alkane except  $i\text{-C}_4\text{H}_{10}$  = 2-methylpropane (isobutane) and  $\text{C}_{30}\text{H}_{62}$  = 2,6,10,15,19,23-hexamethyltetracosane (squalane);  $\text{C}_{10}\text{H}_{18}$  = decahydronaphthalene, *cis* (decalin, *cis*);  $\text{C}_{10}\text{H}_{12}$  = 1,2,3,4-tetrahydronaphthalene (tetralin);  $\text{---}$  = experimental (refs.27,28);  $\circ$  = experimental (ref.49);  $\text{---}$  = calculated (ref.49))

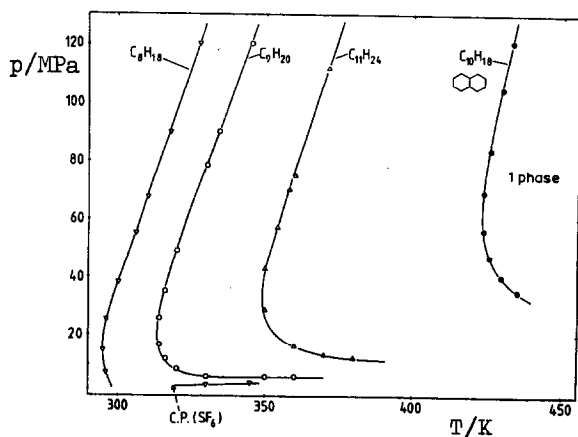


Fig. 15. Critical  $p(T)$  curves of some binary ( $\text{SF}_6$  + hydrocarbon) systems (data from Matzik, refs.32 - 34)

analytical (refs. 35 - 41) method are compiled. For a detailed discussion of these phenomena see ref. 26. With respect to separation methods it is important to know that at temperatures and pressures on the right hand side of the critical  $p(T)$  curves shown the low-volatile component II is miscible with the supercritical solvent I in all proportions whereas for phase separation and layering one has to go back again to the two-phase region beyond the critical

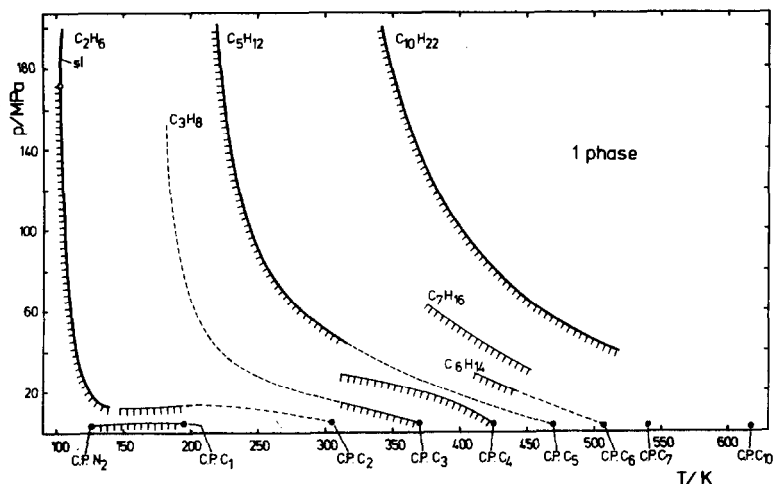


Fig. 16. Critical  $p(T)$  curves of some binary ( $N_2 + n$ -alkane) systems ( $N_2 + C_2H_6$ ,  $N_2 + n-C_5H_{12}$ ,  $N_2 + n-C_{10}H_{22}$  (refs.29,30); all other data are taken from the literature (refs.29,30))

curves.

In Fig. 17 the solvent power of some dense gases with respect to different  $n$ -alkanes is compared. Here the correlation between the UCSTs of binary mixtures of  $CO_2$ ,  $CF_4$ ,  $CHF_3$ , or  $SF_6$  with some members of the homologous series of the  $n$ -alkanes and the chainlengths of the  $n$ -alkanes considered is given for  $p = \text{const}$  (here 50 MPa). Fig. 17 demonstrates that the gases differ considerably in solvent power. Such plots are of interest for the understanding and planning of separations by fluid extraction and supercritical fluid chromatography (SFC). For a detailed discussion see refs. 32,34.

### $p(c)$ Isotherms

For a separation method concentrations  $c_i$  are better composition variables than mole fractions  $x_i$ . The pressure (concentration) isotherms given schematically in Figs. 18c and 18d correspond to the  $p(x)$  isotherms in Figs. 18a and 18b respectively. Here the points A and B which coincide in the  $p(x)$  plots differ by orders of magnitude in concentration in the  $p(c)$  plots. A characteristic example is given in Fig. 19 where some  $p(\log c)$  isotherms (Fig. 19a) and  $\rho(\log c)$  isotherms (Fig. 19b) are presented for  $CO_2 + 2,6,10,15,19,23$ -hexamethyltetracosane (squalane) taken from measurements of Nickel and Swaid (refs. 36,37). From such data so-called enhancement factors

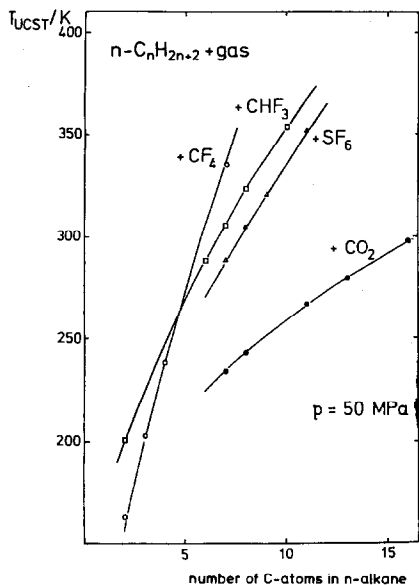


Fig. 17. Correlation between  $T(\text{UCST})$  of binary n-alkane systems with  $\text{CO}_2$ ,  $\text{CF}_4$ ,  $\text{CHF}_3$ , and  $\text{SF}_6$  and the number of C-atoms  $n$  in the alkane ( $p=50 \text{ MPa}$ ).

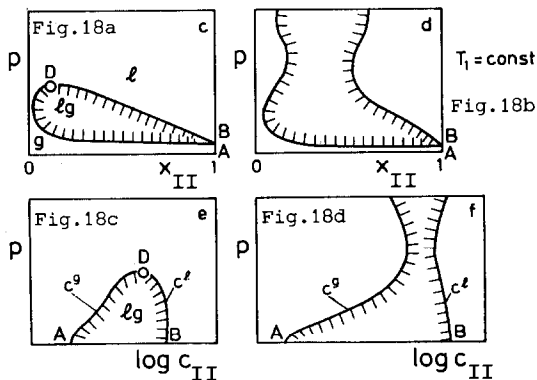


Fig. 18. Pressure (composition) isotherms (schematically)

Figs. 18a and 18b:

$p(x)$  isotherms

Figs. 18c and 18d:

$p(c)$  isotherms

$E \equiv c^g/c^{g*}$  can be calculated where  $c^g$  and  $c^{g*}$  are the concentrations of the low-volatile component II (here squalane) in the fluid solvent I (here  $\text{CO}_2$ ) and above the pure low-volatile substance at its vapour pressure respectively. For the  $\text{CO}_2$  + squalane system  $E$ -values up to  $10^{10}$  are found giving evidence for the rapidly increasing solvent power of supercritical gases with increasing density. For a detailed discussion of these effects especially of the complicated temperature dependence see refs. 26,35 - 37.

#### Calculation of Fluid-Phase Equilibria

Considerable progress was made during the last decade in the calculation and correlation of the phase equilibria of fluid mixtures. An example is given in Fig. 20 where the critical  $p(T)$  curve and one  $p(x)$  isotherm of the system  $\text{CHF}_3$  + octane obtained experimentally (Figs. 13 and 12c) are compared with data that have been calculated from the Redlich-Kwong equation of state by Deiters and Wirths using improved mixing rules (refs.42,43,27,28).

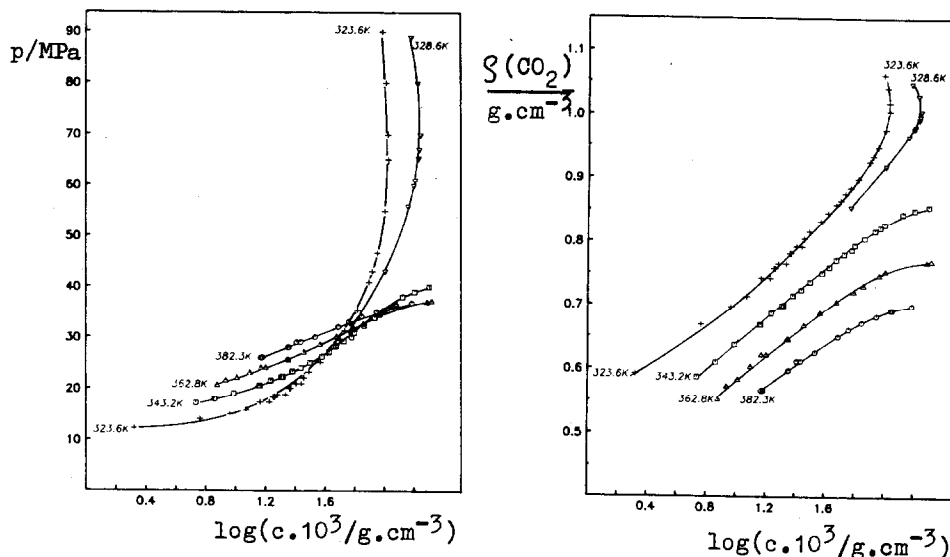


Fig. 19. Pressure (concentration) isotherms (Fig.19a) and density (concentration) isotherms (Fig.19b) for CO<sub>2</sub> + 2,6,10,15,19,23-hexamethyltetracosane (squalane) (data from Nickel and Swaid, refs.36, 37; the abscissa is on a logarithmic scale; the curves given in Fig.19a correspond to the left hand branches of the schematic  $p(c)$  isotherms shown in Figs.18c and 18d)

### Transport Properties

Whereas density and consequently solvent power of supercritical fluid phases are comparable to those of liquids, diffusion coefficients and viscosities resemble more those of gases; as a consequence rather large diffusion coefficients and low viscosities are found. Since the supercritical gas is also soluble in the liquid phase, viscosities and surface tensions are also decreased and diffusion coefficients increased in the liquid equilibrium phase. Most of these phenomena are favourable e.g. for mass transfer. Disadvantageous are the rather high pressures involved, the slowing down of the equilibration rate near critical states, barotropic phenomena, convection etc. For numerical data and a more detailed discussion see refs. 21 - 26.

### Applications

A detailed discussion of the applications of fluid mixtures has been given elsewhere (see refs.14-20). Here only the importance for some new separation methods will be mentioned e.g. for fluid ex-

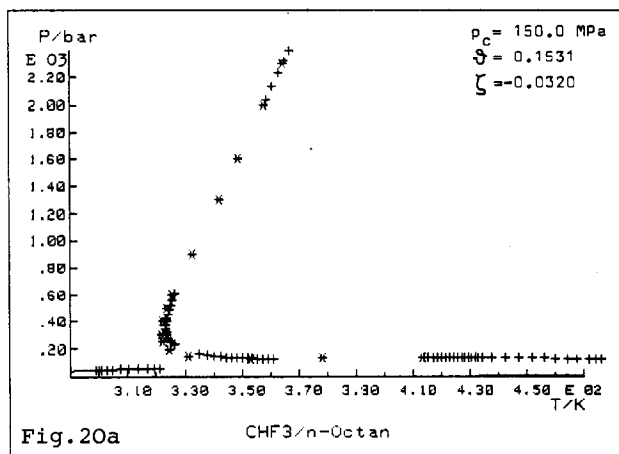


Fig. 20. Calculation of phase equilibria in the system  $\text{CHF}_3 + \text{octane}$  from the Redlich-Kwong equation of state (Deiters and Wirths; refs.27,28, 42,43)

Fig. 20a. Critical  $p(T)$  curve ( $*$  = experimental (see Fig.13),  $+$  = calculated)

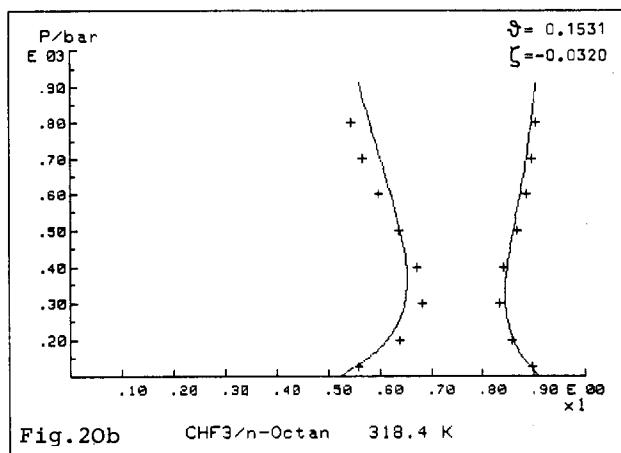


Fig. 20b.  $p(x)$  isotherm at 318.4 K ( $+$  = experimental (see Fig.12c),  $—$  = calculated)

traction (e.g. caffeine, hops, spices, drugs, nicotine, fragrances, soy-beans, oil-seeds, ethanol, coal, wood, lubricants etc) or supercritical fluid chromatography (SFC) (especially for analytical and preparative applications and for the determination of physicochemical properties e.g. capacity ratios, diffusion coefficients). These and other applications have been extensively discussed in some books (refs. 14,15) and the proceedings of some meetings (see refs. 16 - 20,23).

For some large-scale high-pressure processes in industry (e.g. oxo synthesis, LDPE), the importance of highly compressed fluid mixtures will probably decrease in the future since efforts are made to use lower or normal pressures in order to save compression costs. The interest in fluid mixtures with respect to geothermal energy production, tertiary oil recovery, gasification and lique-



faction of coal etc, however, will increase considerably. For (relatively smallscale) extractions of rather expensive substances (e.g. natural products such as caffeine, hops, drugs, spices, fragrances etc) fluid extraction will remain a promising technique. Experimental investigations and theoretical description of fluid mixtures as a function of temperature, pressure and composition are and will be a challenge for scientists and engineers.

#### ACKNOWLEDGEMENTS

The author thanks the Organizers of the Conference, the Society of Calorimetry and Thermal Analysis of Japan and the Japan Society for the Promotion of Science for having invited him. He expresses his gratitude to his collaborators at the University of Bochum who have produced the data presented in this review - A. Bartelt, Dr. J. Herrmann, Dr. H.D. Kleinmans, H. Reisig, and A. Rotherth with respect to the work on liquid crystals - Dr. I. Matzik, D. Nickel, Dr. R. Paas, Dr. K. Peter, Dr. I. Swaid, Dr. M. Wirths, and Dr. K.D. Witsotzki with respect to the work on fluid mixtures - Dr. D. Bartmann, R. Feist, A. Kopner, Dr. U. van Wasen, and A. Wilsch with respect to the work on supercritical fluid chromatography (SFC). Financial support of the investigations from the Deutsche Forschungsgemeinschaft (DFG), the Minister für Wissenschaft und Forschung Nordrhein-Westfalen and the Fonds der Chemischen Industrie e.V. is gratefully acknowledged.

#### REFERENCES

- 1 G.M. Schneider, this issue.
- 2 M. Sorai, this issue.
- 3 C.W. Garland, this issue.
- 4 S. Chandrasekhar, R. Shashidhar, *Advances in Liquid Crystals* 4 (1979) 83-120.
- 5 J. Herrmann, *Doctoral Thesis, University of Bochum, 1983.*
- 6 H.D. Kleinmans, *Doctoral Thesis, University of Bochum, 1984.*
- 7 H. Reisig, *Diploma Thesis, University of Bochum, 1983.*
- 8 A. Bartelt, *Diploma Thesis, University of Bochum, 1984.*
- 9 H.D. Kleinmans, G.M. Schneider, *Thermochimica Acta* 69 (1983) 229-234.
- 10 H.D. Kleinmans, R. Konrad, G.M. Schneider, *Thermochimica Acta* 69 (1983) 317-374.
- 11 J. Herrmann, H.D. Kleinmans, G.M. Schneider, *J.Chim.Phys.Chim. Biol.* 80 (1983) 111-117.
- 12 J. Herrmann, A. Bartelt, H.D. Kleinmans, H. Reisig, G.M. Schneider, *Mol. Cryst.Liq.Cryst.Letters* 92 (1983) 225-230.
- 13 A. Bartelt, H. Reisig, J. Herrmann, G.M. Schneider, *Mol.Cryst. Liq.Cryst.Letters*, in press.
- 14 G.M. Schneider, E. Stahl, G. Wilke (Eds.), *Extraction with Supercritical Gases*, Verlag Chemie, Weinheim, 1980.
- 15 M.E. Paulaitis, J.M.L. Penninger, R.D. Gray Jr., P. Davidson, *Chemical Engineering at Supercritical Conditions*, Ann Arbor

- Science Publishers, Michigan, 1983.
- 16 K.D. Timmerhaus, M.S. Barber (Eds.), High Pressure Science and Technology, Vol.1, Plenum Press, New York, 1979, 506-608.
  - 17 Angew. Chem. Int. Ed. Engl. 17 (1978) 701-754.
  - 18 Sep. Sci. Techn. 17 (1982) 1-287.
  - 19 Fluid Phase Equil. 10 (1983) 135-358.
  - 20 Ber. Bunsenges. Phys. Chem. 88 (1984) 784-922.
  - 21 G.M. Schneider, Angew.Chem.Int.Ed.Engl. 17 (1978) 716-727.
  - 22 G.M. Schneider, in Chemical Thermodynamics, Vol.2 (M.L. McGlashan Ed.), A Specialist Periodical Report, London, 1978, Chap.4.
  - 23 U. van Wasen, I. Swaid, G.M. Schneider, Angew.Chem.Int.Ed.Engl. 19 (1980) 575-587.
  - 24 G.M. Schneider, Fluid Phase Equil., 10 (1983) 141-157.
  - 25 G.M. Schneider, Pure & Appl. Chem., 55 (1983) 479-492.
  - 26 G.M. Schneider, Ber.Bunsenges.Phys.Chem. 88 (1984) 841-848.
  - 27 M. Wirths, Doctoral Thesis, University of Bochum, 1983.
  - 28 M. Wirths, G.M. Schneider, Fluid Phase Equil., in press.
  - 29 K.D. Wisotzki, Doctoral Thesis, University of Bochum, 1984.
  - 30 K.D. Wisotzki, G.M. Schneider, Ber.Bunsenges.Phys.Chem., in press.
  - 31 M. Wirths, K.D. Wisotzki, Ber.Bunsenges.Phys.Chem.88(1984)921.
  - 32 I. Matzik, Doctoral Thesis, University of Bochum, 1984.
  - 33 I. Matzik, Ber.Bunsenges.Phys.Chem. 88 (1984) 921.
  - 34 I. Matzik, G.M. Schneider, Ber.Bunsenges.Phys.Chem., in press.
  - 35 I. Swaid, Doctoral Thesis, University of Bochum, 1984.
  - 36 I. Swaid, D. Nickel, Ber.Bunsenges.Phys.Chem. 88 (1984) 920.
  - 37 I. Swaid, D. Nickel, G.M. Schneider, Fluid Phase Equil., in press.
  - 38 R. Konrad, Doctoral Thesis, University of Bochum, 1982.
  - 39 R. Konrad, I. Swaid, G.M. Schneider, Fluid Phase Equil. 10 (1983) 307-314.
  - 40 G. Katzenski, R. Konrad, Ber.Bunsenges.Phys.Chem. 88 (1984) 921.
  - 41 G. Katzenski, Doctoral Thesis, University of Bochum, in press.
  - 42 U.K. Deiters, G.M. Schneider, Ber.Bunsenges.Phys.Chem. 80 (1976) 1316-1324.
  - 43 U.K. Deiters, I. Swaid, Ber.Bunsenges.Phys.Chem. 88 (1984) 791-796.
  - 44 A. Wilsch, R. Feist, G.M. Schneider, Fluid Phase Equil. 10 (1983) 299-306.
  - 45 A. Wilsch, G.M. Schneider, Fresenius Z.Anal.Chem. 316 (1983) 265-267.
  - 46 A. Wilsch, Doctoral Thesis, University of Bochum, in preparation.
  - 47 R. Feist, Doctoral Thesis, University of Bochum, in preparation.
  - 48 A. Kopner, R. Feist, Ber.Bunsenges.Phys.Chem. 88 (1984) 922.
  - 49 J.M.M. Mendonça, Ph.D.Thesis, Imperial College, London, 1979.
  - 50 D. Nickel, Diploma Thesis, University of Bochum, 1984.
  - 51 A. Rotherth, Diploma Thesis, University of Bochum, 1984.